

# MICROCRYSTALLINE SILICON SOLAR CELLS: THEORY AND DIAGNOSTIC TOOLS

Fanny Meillaud, Arvind Shah, Julien Bailat, Evelyne Vallat-Sauvain, Tobias Roschek<sup>1,2</sup>, Bernd Rech<sup>1</sup>, Didier Dominé, Thomas Söderström, Martin Python, Christophe Ballif  
 Institut de Microtechnique de l'Université, CH-2000 Neuchâtel, Switzerland  
<sup>1</sup>Institute of Photovoltaics, Forschungszentrum Juelich GmbH, D-52425 Juelich, Germany  
<sup>2</sup>Unaxis A.G., Solar Division, Trübbach (SG), Switzerland

## ABSTRACT

A simple theoretical model for pin/nip-type  $\mu\text{c-Si:H}$  solar cells is presented. It is based on a superposition of a drift-dominated collection model and of the classical drift-diffusion transport model of the pn-diode. The model is the basis for a solar cell equivalent circuit, identical to the one introduced by Merten et al. [1], for amorphous cells. The equivalent circuit serves as framework for the diagnosis of faulty solar cells, by selected experimental tools, such as: J(V) curves, Quantum efficiency (QE) curves, Raman spectroscopy, Fourier-Transform Photo Spectroscopy (FTPS), Variable Intensity Measurements (VIM) [1]. The main parameter that characterizes solar cell "quality" is the fill factor (FF). For best cells FF is over 75%. FF can be reduced by (1) collection problems (characterized by a drop in the collection voltage  $V_{\text{coll}}$ ); (2) shunts (characterized by low shunt resistance  $R_{\text{shunt}}$ ); (3) excessive series resistance. Thanks to VIM analysis, it is possible to discriminate experimentally between these 3 types of deficiencies. It is also possible to measure  $V_{\text{coll}}$  very easily and link it to fill factor reduction  $\Delta\text{FF}$ . Selected examples of solar cell series and case studies of defective and degraded cells are given.

## 1. Theoretical Model and Equivalent Circuit

In extension of earlier work [1] on amorphous silicon (a-Si:H) solar cells, a simple model is proposed here for  $\mu\text{c-Si:H}$  solar cells: It is based on adding collection current density  $J_{\text{coll}}$ , and diode current density  $J_{\text{diode}}$

$$J_{\text{total}} = J_{\text{coll}} + J_{\text{diode}} \quad (1)$$

$J_{\text{diode}}$  is given by the drift-diffusion diode model

$$J_{\text{diode}} = J_0 \{ \exp(q V_{\text{appl}} / nkT) - 1 \} \quad (2)$$

For p-i-n diodes:  $J_{\text{coll}} = J_{\text{gen}} - J_{\text{rec}} - J_{\text{shunt}}$  (3),

with  $J_{\text{rec}} \approx J_0 (d_i / l_{\text{drift}})$  (4)

$J_{\text{gen}}$  is the photogenerated current density, which is, in its turn, proportional to the intensity of incoming light

$J_{\text{rec}}$  is the recombination current density,

$l_{\text{drift}} = (\mu\tau_{\text{eff}} \times E_{\text{eff}})$  is the drift length within the i-layer

$J_{\text{shunt}} \approx V_{\text{appl}} / R_{\text{shunt}}$  is the current density through physical micro-shunts (resistance  $R_{\text{shunt}}$ ),

$\mu\tau_{\text{eff}}$  the effective mobility x lifetime product of the i-layer,

$E_{\text{eff}} \approx \{(V_{\text{bi}} - V_{\text{appl}}) / \Psi d_i\}$  the effective electric field within the i-layer  $\{\Psi$  is a "form factor" taking into account the deformation of the electric field  $E(x)$  [2], p. 64  $\}$ ,  $V_{\text{bi}}$  is the built-in voltage,  $V_{\text{appl}}$  the external applied voltage,  $d_i$  the i-layer thickness,  $J_0$  the diode reverse saturation current density,  $n$  the diode ideality factor,  $q$  the unit charge,  $k$  the Boltzmann constant and  $T$  the absolute temperature.

$E_{\text{eff}}$  is reduced by space charge: e.g. by ionised contaminants (O, B) and charged defects.

At  $V_{\text{appl}} = 0$ , eq. (4) becomes:  $J_{\text{rec}} \approx J_{\text{gen}} (V_{\text{bi}}/V_{\text{coll}})$ , where  $V_{\text{coll}}$  is called the "collection voltage" (see below).

This model leads to the equivalent circuit of Fig. 1:

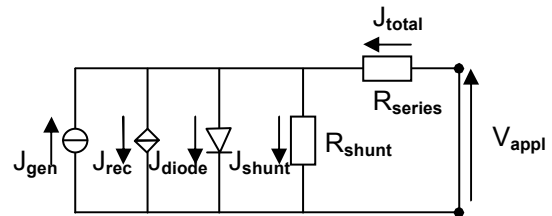


Fig.1 Equivalent circuit for pin-type solar cells [1]; the **controlled** current sink  $J_{\text{rec}}$  (equation (4)) depends on i-layer "quality",  $R_{\text{shunt}}$  originates from micro-shunts at the edges or in the bulk of the cell;  $R_{\text{series}}$  is given by contacts and TCO; the diode D is represented by eq. (3), and characterized by  $J_0$  and  $n$ , where  $J_0$  is given by material band gap, defect density  $N_{\text{defect}}$  and by cell thickness  $d_i$ .

The circuit of Fig. 1 is too complex for electrical system design; it is, however, useful for cell diagnostics, because it splits up the "usual" parallel resistance  $R_p$  of the "classical" equivalent circuit into 2 parts: recombination losses ( $J_{\text{rec}}$ ) and "true", physical micro-shunts ( $R_{\text{shunt}}$ ).

## 2. Package of Diagnostic Tools

The following measurement methods have been used to investigate microcrystalline silicon solar cells and to diagnose faults in design and fabrication that may have limiting effects on solar cell performance:

- classical  $J(V)$  curves at  $100 \text{ mW/cm}^2$ ,
- External Quantum Efficiency curves  $\{EQE(h\nu)\}$ , at different values of the bias voltage  $V_{\text{bias}}$ ,
- Raman spectroscopy ( $\rightarrow$  "Raman crystallinity"  $X_c$ ),
- Fourier-Transform Photocurrent Spectroscopy (FTPS), giving absorption  $\alpha(h\nu)$ , preferably on a  $\log \alpha$  - plot,
- Variable Intensity Measurements (VIM), i.e.  $J(V)$  curves at  $0.001 - 100 \text{ mW/cm}^2$ .

Raman (used here at 633 nm) allows one to evaluate i-layer crystallinity, **after** fabricating the solar cell [3].

FTPS gives us i-layer defect density  $\{\text{via } \alpha(0.8 \text{ eV})\}$  and structural disorder  $\{\text{via the Urbach energy } E^0, \text{ i.e. via the slope of the band-edge in the } \log \alpha(h\nu) \text{ plot}\}$ ; it is also measured on entire pin/n-i-p cells, **after** fabrication [4].

EQE ( $h\nu, V_{\text{bias}}$ ) gives information on collection within the i-layer; the latter is also determined by VIM (by evaluating  $V_{\text{coll}}$ ). VIM [1] gives additional insight into  $R_{\text{shunt}}$  and  $R_{\text{series}}$ : two critical parameters in thin-film silicon cells.

Table 1 shows the **Ideal** values obtained today for  $\mu\text{-Si-Si:H}$  i-layers and state-of the art (best)  $\mu\text{-Si-Si:H}$  solar cells, after carefully tailoring the plasma reactors to the needs of  $\mu\text{-Si-Si:H}$  deposition, and after mastering all steps of cell fabrication. It also shows the **Range** of values that are easily obtained, by transferring deposition systems and other fabrication steps, as they are used for a-Si:H cells, and just increasing  $\text{H}_2$  dilution, to obtain  $\mu\text{-Si-Si:H}$ .

Parameter	Ideal	Range
Raman crystallinity $X_c$	60%	30 $\rightarrow$ 80 %
Defect absorption $\alpha$ (0.8 eV)	0.01	0.1 $\rightarrow$ 10 $\text{cm}^{-1}$
Urbach energy $E^0$	35	
EQE (0 V) @ 450 nm	70%	
EQE (0 V) @ Max ( $\approx 570 \text{ nm}$ )	85%	
EQE (0 V) @ 700 nm	80%	
EQE (0 V) @ 850 nm	50%	
$R_{\text{shunt}}$ [ $\text{k}\Omega\text{cm}^2$ ]	100	1 $\rightarrow$ 10
$R_{\text{series}}$ [ $\Omega\text{cm}^2$ ]	5	5 $\rightarrow$ 10
Collection voltage	80 V	20 $\rightarrow$ 75 V
$V_{\text{coll}} = \mu\tau_{\text{eff}}/\Psi \cdot (V_{\text{bi}}/d_i)^2$		

Table 1 Typical parameters for microcrystalline silicon layers/cells, as currently reported in the literature: "**Ideal**" values refer to best published data; "**Range**" refers to data published, in general, by many groups (see text).

## 3. Analyzing the Fill Factor

For  $\mu\text{-Si-Si:H}$  solar cells, the "ideal" calculated value of FF (given by the 1.1 eV band gap of  $\mu\text{-Si-Si:H}$  [5]) is over 75%; however, in practice, cells often exhibit values in the 60 to 70 % range. In thin-film silicon solar cells, there are 3 main reasons why FF is reduced to values below its limit value: (A) recombination losses within the i-layer and at the p/i and i/n interfaces; (B) partial micro-shunts through the i-layer (and through the whole cell); (C) contact and doped layers with too high resistivity. In the equivalent circuit of Fig. 1, effect (A) increases  $J_{\text{rec}}$ , by decreasing the collection voltage  $V_{\text{coll}} = \mu\tau_{\text{eff}}/\Psi \cdot (V_{\text{bi}}/d_i)^2$ ; effect (B) decreases  $R_{\text{shunt}}$ ; effect (C) increases  $R_{\text{series}}$ .

In case (A) the value of FF is reduced and  $J_{\text{rec}}$  increased, as shown schematically in Fig.2, under the assumption that the maximum power point (MPP) remains at the same value of  $V$ , when recombination increases

In practice it is important to analyze why the FF of a given cell is low. Here, VIM analysis can help:

Plot  $\log R_{\text{sc}} = f\{\log(J_{\text{sc}}^{-1})\}$ , as in Fig. 3. (For the definition of  $1/R_{\text{sc}}$ , see Fig.2.) The slope of the  $\log R_{\text{sc}}$ -curve is indeed equal to  $V_{\text{coll}}$ ; the curve itself goes asymptotically towards  $R_{\text{shunt}}$ , for  $J_{\text{sc}} \rightarrow 0$ . The asymptote for  $J_{\text{sc}} \rightarrow \text{infinity}$  would give  $R_{\text{series}}$  but is difficult to locate, unless very high light intensities ( $\gg 1$  sun) are used.

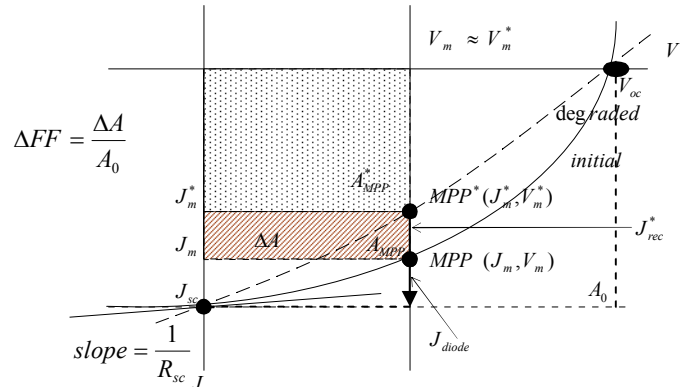


Fig. 2 Schematic representation of  $J(V)$  curves for ideal cell and cell with strong recombination losses  $J_{\text{rec}}$ .

The following relationship (from [5]) links the collection voltage  $V_{\text{coll}} = V_{\text{bi}} \text{ l}_{\text{drift}} / d_i$  to the fill factor reduction:

$$\Delta FF \approx \frac{V_{\text{bi}}}{V_{\text{coll}}} \cdot 90\% , \quad (5)$$

As  $V_{\text{bi}}$  is around 1V, a collection voltage  $V_{\text{coll}}$  of only 10 V, as is often encountered with "medium-quality"  $\mu\text{-Si-Si:H}$  i-layers, will lead to a FF reduction of 9 % ( $\rightarrow 66\%$ ) !

Note: The determination of  $V_{\text{coll}}$  (by VIM) is probably the easiest way to determine the "quality" of the i-layer.

#### 4. Investigation of selected solar cells

##### (a) Variable gas flow series

Above diagnostic tools were applied to a series of  $\mu\text{-Si:H}$  solar cells deposited by Roschek et al. [6] under “high pressure depletion (HPD)” conditions. HPD allows one to increase the deposition rate, whilst maintaining i-layer quality. However, HPD generally requires high gas flows, especially high  $\text{H}_2$  flows: economically, this can be a serious disadvantage. In the series investigated here, Roschek et al. [6] therefore fabricated  $\mu\text{-Si:H}$  solar cells under HPD conditions, at 13.56 MHz, but with step-wise reduced  $\text{H}_2$  flow rates; the  $[\text{H}_2]:[\text{SiH}_4]$  dilution ratio was adjusted in such a way, as to keep Raman crystallinity  $X_c$  constant, at about 60%. One notices (Table 2) that FF drops from 72% to 66% when the  $\text{H}_2$  flow rate is reduced from 750 sccm to 50 sccm. The main reason for this drop can be revealed by (a) VIM and (b) FTPS measurements (see Fig. 3 and Table 2): It is an increase in i-layer defect density. However,  $V_{\text{coll}}$  suffers a stronger reduction than  $\{\alpha(0.8 \text{ eV})\}^{-1}$ . This may be explained by stronger O-incorporation at lower gas flow rates, leading to field deformation (increase in  $\Psi$ ) and lower  $E_{\text{eff}}$ .

$\text{H}_2$ flow [sccm]	750	50
i-layer thickness [ $\mu\text{m}$ ]	1.29	1.09
$X_c$ [%]	66.5	60.0
$J_{\text{sc}}$ [ $\text{mA}/\text{cm}^2$ ]	21.9	21.8
EQE (@700 nm, 0V)	0.70	0.72
EQE (@ 700nm, -1.5 V)	0.70	0.74
$R_{\text{shunt}}$ [ $\text{k}\Omega\text{cm}^2$ ]	140	25
$V_{\text{oc}}$ [mV]	538	497
FF [%]	72.4	66.2
$V_{\text{coll}} = \mu\tau_{\text{eff}}/\Psi \cdot (V_{\text{bi}}/d_i)^2$ [V]	59.4	12.5
$\mu\tau_{\text{eff}}$ [ $\text{cm}^2/\text{V}$ ]	$8.0 \cdot 10^{-7}$	$1.1 \cdot 10^{-7}$
$\alpha$ (0.8 eV) [ $\text{cm}^{-1}$ ]	$2.5 \cdot 10^{-3}$	$4.4 \cdot 10^{-3}$
$E_0$ [meV]	35.8	39.6

Table 2 Solar cell parameters for 2 cells of the variable gas flow series: a “good” cell at 750 sccm  $\text{H}_2$  flow and a “poor” cell at 50 sccm. Table 2 does not aim at showing the limits of the HPD deposition method. Its only aim is to show how solar cell parameters are affected when i-layer quality is reduced. (Note: There are indeed many publications in the last PV conferences, which address the issue of fabricating excellent  $\mu\text{-Si:H}$  solar modules at higher deposition rates and with reasonable gas usage.)

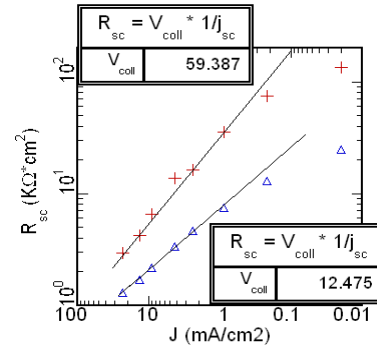


Fig. 3 VIM analysis for 2 cells of the variable gas flow series; the curves for  $\log R_{\text{sc}} = f\{\log(J_{\text{sc}}^{-1})\}$  have, for intermediate values of  $J_{\text{sc}}$ , slopes that are equal to  $V_{\text{coll}}$ ; the curves tend asymptotically towards  $R_{\text{shunt}}$ , for  $J_{\text{sc}} \rightarrow 0$ .

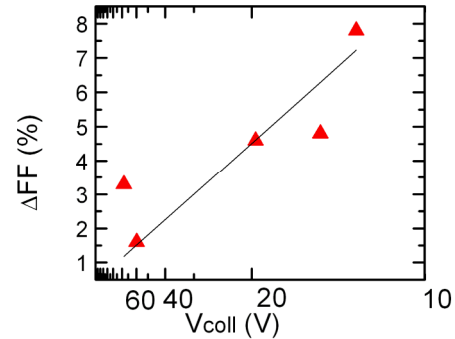


Fig. 4  $\Delta\text{FF}$  as a function of  $V_{\text{coll}}$ ; points marked as  $\Delta$  are measured values for the variable gas flow series; straight line is a theoretical prediction according to eq. (5); here  $\Delta\text{FF} = \text{FF}_0 - \text{FF}$ , where  $\text{FF}_0 = 75\%$

##### (b) Light-induced degradation

Microcrystalline solar cells have a mild form of light-induced degradation or “Staebler-Wronski Effect (SWE)”. The degradation effect is (relatively) lower for cells with a high value of Raman crystallinity. Cells with intermediate crystallinity ( $X_c \approx 50\%$ ) show (in absolute terms) the best performance, both in the initial and in the degraded state [5, 7]: This is linked to a minimum in  $\alpha$  (0.8 eV) and in  $J_{\text{rec}}$ , and to a maximum in both  $\mu\tau_{\text{eff}}$  and  $V_{\text{coll}}$ . Light-induced degradation manifests itself, in general, by an increase in  $\alpha$  (0.8 eV) and by corresponding variations in  $V_{\text{coll}}$ ,  $\mu\tau_{\text{eff}}$  and  $J_{\text{rec}}$ . Most other solar cell parameters are hardly affected [7]. Table 3 and Fig. 5 illustrate this.

	Before	After
Raman crystallinity $X_c$	50%	
$J_{sc}$ (mA/cm <sup>2</sup> )	18.3	18.0
EQE (@700 nm, 0V)	0.50	0.49
EQE (@ 700nm, -1.5 V)	0.55	0.54
$V_{oc}$ [mV]	527	525
FF [%]	66.2	63.9
$R_{shunt}$ [k $\Omega$ cm <sup>2</sup> ]	170	140
$V_{coll} = \mu\tau_{eff}/\Psi \cdot (V_{bi}/d_i)^2$ [V]	14.2	10.1
$\mu\tau_{eff}$ [cm <sup>2</sup> /V]	$4.3 \cdot 10^{-7}$	$3.0 \cdot 10^{-7}$
$\alpha$ (0.8 eV) [cm <sup>-1</sup> ]	$2.6 \cdot 10^{-3}$	$4.6 \cdot 10^{-3}$
$E_0$ [meV]	36.2	36.4

Table 3 Solar cell parameters for a typical pin cell (2  $\mu$ m thick,  $X_c \approx 50\%$ ), before/after light-soaking. Note the drop in  $V_{coll}$  from 14.2 to 10.1 V, corresponding to an increase in  $\Delta FF$  from 6.3 to 8.9%, according to eq. (5).

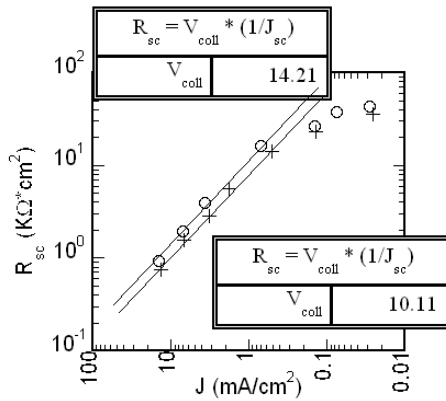


Fig. 5 VIM analysis for the cell of Table 3 (dilution series,  $X_c \approx 50\%$ ), before  $\bullet$  and after  $+$  light-soaking (see Fig. 3 for explanations about VIM analysis)

### (c) Micro-shunts

Microcrystalline solar cells are often afflicted by micro-shunts (which can be seen by VIM, as illustrated in Fig.6); such micro-shunts lead often to a reduction in FF, according to the following equation [5]:

$$\Delta FF = R_{equ}/R_{shunt} \quad (6),$$

with

$$R_{equ} \approx 2 \text{ k}\Omega\text{cm}^2;$$

$$R_{shunt} \text{ in [k } \Omega\text{cm}^2], \Delta FF \text{ in } \%$$

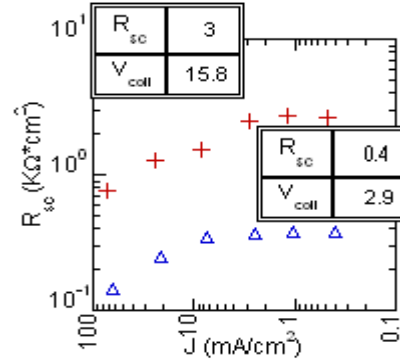


Fig. 6 VIM analysis for 2 typical  $\mu$ c-Si:H cells with micro-shunts (a) lightly shunted  $+$ , i.e.  $R_{shunt} = 3 \text{ k}\Omega\text{cm}^2$ ; the FF at AM 1.5 is almost not affected; (b) heavily shunted  $\Delta$ ,  $R_{shunt} = 0.4 \text{ k}\Omega\text{cm}^2$ ; at AM 1.5  $\Delta FF = 4.5 \%$ , by comparison with a non-shunted cell of the same run.

## CONCLUSIONS

For microcrystalline silicon solar cells adequate diagnostic tools, such as Raman and FTPS are important. A standard indicator for cell performance is the fill factor (FF). Because of the frequent occurrence of cracks and shunts in microcrystalline layers, it is particularly important to analyze whether a low value of FF is due to low shunt resistance  $R_{shunt}$  or to increased recombination, i.e. to a low value of the "collection voltage"  $V_{coll}$ . This can be done by VIM.  $V_{coll}$  turns out to be a key parameter to evaluate the "quality" of the i-layer within entire cells. With spectrally-resolved VIM it should, in future, also be possible to separate the effects of bulk and interfaces.

## ACKNOWLEDGEMENTS

Support was given by FNSRS, grant FN200021-107469.

## REFERENCES

- [1] J. Merten et al., *IEEE Transactions on Electron Devices*, **ED-45**, 1998, pp. 423-429
- [2] C. Hof, *Ph.D. thesis*, Univ. of Neuchâtel, 2000.
- [3] J. Bailat et al., *J. Appl. Phys.*, **93**, 2003, pp. 5727-5732,
- [4] A. Poruba et al., *J. Non-Crystalline Solids*, **299-302**, 2002, pp. 536-540.
- [5] F. Meillaud, *Ph.D. thesis*, Univ. of Neuchâtel, 2006.
- [6] T. Roschek et al., *Thin Solid Films*, **451-452**, 2004, pp. 466-499
- [7] F. Meillaud et al., *Proc. of the 20<sup>th</sup> EU PVSEC*, ISBN 3-936338-19-1, 2005, pp. 1509-1512.